

# Identification and Control of Unbalance and Sensor Runout on Rigid by Active Magnetic Bearing Systems

Yoichi Kanemitsu, Sinya Kijimoto, Koichi Matsuda, Park Tea Jin  
Department of Intelligent Machinery and systems, Graduate School of Engineering,  
Kyushu University, JAPAN E-mail:kanemitu@mech.kyushu-u.ac.jp

## ABSTRACT

In this paper, we propose a new identification method of the sensor runout and the unbalance on a rigid rotor supported by active magnetic bearings applying the incremental least square on-line method and perform some numerical simulations and experiments on the their identification applying to a rigid rotor model of a turbo-molecular pump. The paper also presents some results of the experiment on the identification accuracy and effects of the rotor model error. From the numerical simulations and the experiments, we conclude that the proposed identification method is effective for the simultaneous identification of the unbalance of rotor and the sensor runout.

## 1 INTRODUCTION

An active magnetic bearing(AMB) is non-contact, frictionless and has the ability to actively control the bearing force and the journal eccentricity in the bearing. The application of AMB also has a possibility to compensate the mass unbalance on the rotor.

Two methods are generally adopted to reduce the unbalance vibration of the rotor levitated by AMB. One method is called the peak-gain method (PG method), in which the feedback gain of the AMB controller is extremely high only at the rotating speed frequency. Another method is called the feed forward method (FF method)<sup>(1)</sup> in which the unbalance on the rotor is estimated from the measured vibration signals by the AMB proximity sensor and a compensating magnetic pull from the AMB is added to the rotor in opposite direction of the unbalance force so as to cancel out the mass unbalance force. The FF Method is better than the PG method from the viewpoint of system stability. But it is essential to estimate the unbalance correctly for the FF method.

In a magnetically levitated rotor by AMB, the clearance between rotor and stator is usually measured by the eddy current type proximity sensor, which is sensitive to circumferential irregularity of conductivity and permeability of sensor target material on the rotor. The measured signal by the sensor is called electrical sensor runout<sup>(2)</sup>. The proximity sensor runout enters into the control circuit of the AMB and then the magnetic pull induced by the runout signal whirls the rotor supported the AMB just as an unbalance on the rotor does. And moreover the undesirable sensor runout saturates the control current from the power source.

It is necessary for realization of minimal rotor whirl by the FF method to identify the sensor runout and the unbalance at the same time, compensate the unbalance force by the FF method and eliminate the sensor runout from the measured proximity signal of the AMB simultaneously. It is recommended for minimization of the control current to use the modified proximity signal without the runout for the AMB levitation control.

## 2. EQUATION OF MOTION OF RIGID ROTOR SUPPORTED BY ACTIVE MAGNETIC BEARINGS

A simple AMB model is shown in figure 1. AMB levitates a rotor by regulating the current in magnetic coil and holding the bearing clearance (gap) constant. An attractive force from AMB is formulated as Equation(1).

$$f = -\frac{\mu_0 SN^2}{8} \cdot \left( \frac{i_{p0} + i}{x_{p0} + x} \right)^2 + \frac{\mu_0 SN^2}{8} \cdot \left( \frac{i_{n0} - i}{x_{n0} - x} \right)^2 = \frac{\mu_0 SN^2}{8} \cdot \left\{ -\left( \frac{i_{p0} + i}{x_{p0} + x} \right)^2 + \left( \frac{i_{n0} - i}{x_{n0} - x} \right)^2 \right\} \quad (1)$$

Equation (1) is linearized with respect to the control current  $i$  and the gap change  $x$  as follows:

$$f = -Fi + Gx$$

where

$$F = \frac{\mu_0 SN^2}{4} \left\{ \frac{i_{p0}}{x_{p0}^2} + \frac{i_{n0}}{x_{n0}^2} \right\}, \quad G = \frac{\mu_0 SN^2}{4} \left\{ \frac{i_{p0}^2}{x_{p0}^3} + \frac{i_{n0}^2}{x_{n0}^3} \right\}$$

$F, G$  are called AMB control stiffness and negative position stiffness respectively.

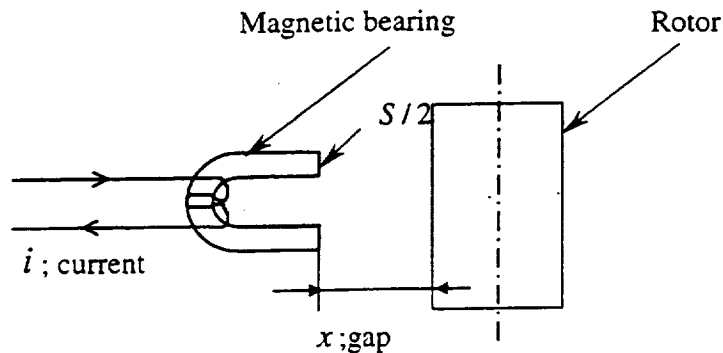


Figure 1 A Model of Active Magnetic Bearing

In this paper, we try to identify the unbalance and the sensor runout on a rotor of a small turbo-molecular pump levitated by AMB, of which photograph is shown in figure 2.

In order to make a numerical model of AMB, the transfer function of the controller has been measured and approximated with PID type controller which is represented as Equation (2) and the measured and the esti-

mated transfer functions are shown in figure 3. The solid line and the dotted line represent the measured transfer function and the approximated one. The estimated PID gain is also tabulated in table 1.

$$i = k_p \hat{x} + k_i \int \hat{x} dt + k_d \frac{d\hat{x}}{dt} \quad (2)$$

The rotor of the turbo-molecular pump is levitated by 2 AMBs and has a massive cylinder with rotor blades on the top end. Now the cylinder is replaced by a disk for the convenience of the verification experiment of the proposing identification method. The tested rotor is drawn in figure 4.

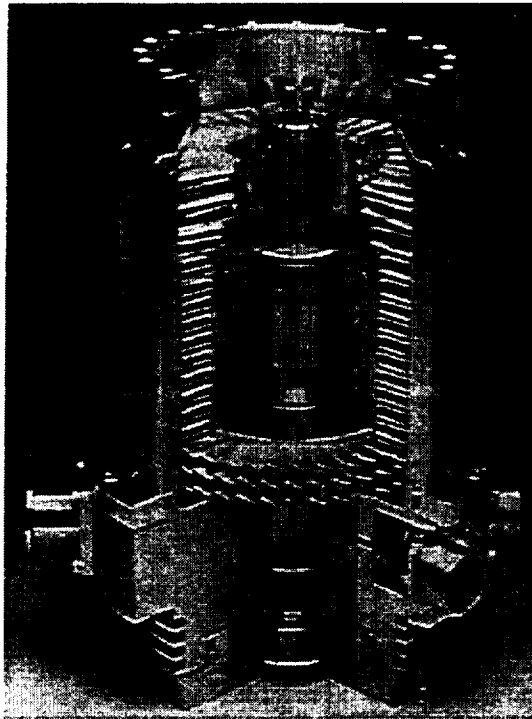


Figure 2 Photograph of the turbo molecular pump rotor

Table 1 Estimated control gain of AMB from measured transfer function

	Bearing 1	Bearing 2
$k_p$ (A/m)	7810	6950
$k_i$ (A/ms)	98300	49300
$k_d$ (As/m)	9.83	4.4

Equation of motion of the rigid rotor shown in figure 4 and levitated by 2 AMBs is given as following equation.

$$M\ddot{x} + \omega M_1 \dot{x} + F_i + Gx_i = U_i \quad (3)$$

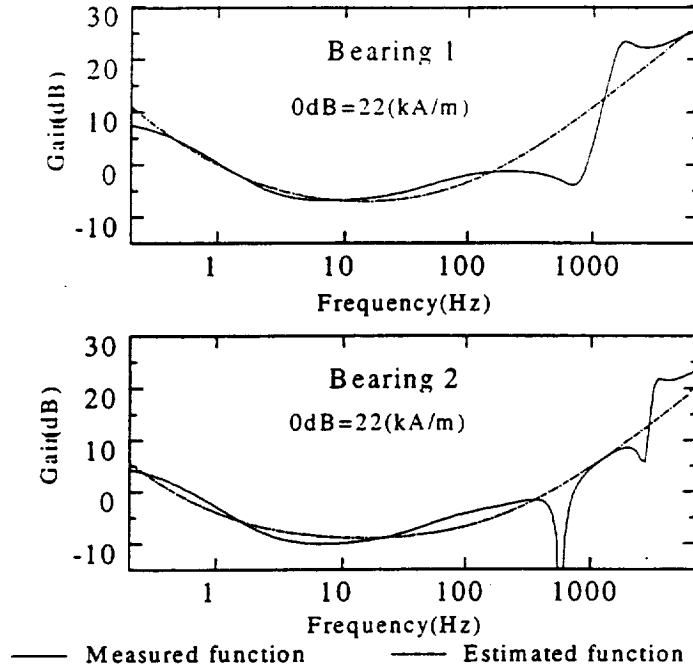


Figure 3 Measured and estimated transfer function

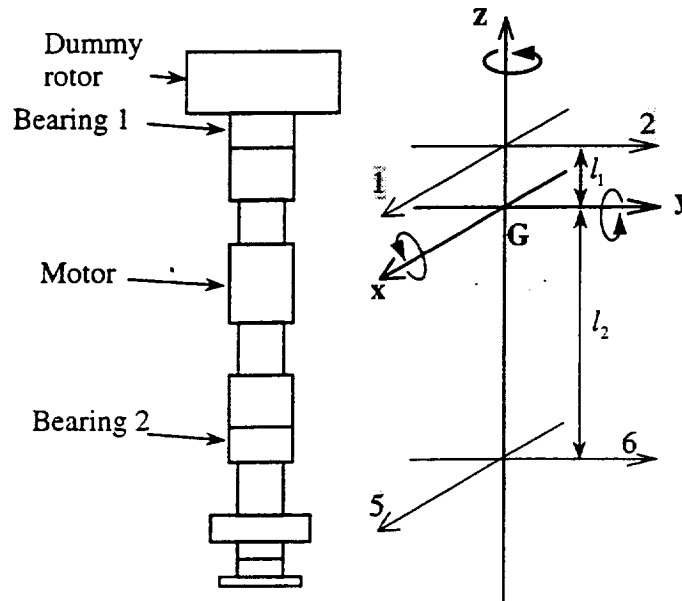


Figure 4 Rotor Model of Turbo-molecular Pump

(1,2,5,6 indicate the upper bearing in x direction and y-direction and the the lower bearing x-direction and y-direction respectively. G is the center of gravity of the rotor)

where  $\mathbf{x}, \mathbf{x}_s, \mathbf{x}_r, \mathbf{i}$  are the actual rotor displacement vector, the measured displacement vector at AMB sensor, the sensor runout vector and the AMB control current vector.  $\mathbf{M}, \mathbf{M}_1, \mathbf{U}_i, \mathbf{F}, \mathbf{G}$  are the mass matrix, the gyro-moment matrix, the rotor unbalance matrix, the control stiffness matrix and the negative position stiffness matrix.

$$\begin{aligned} \mathbf{x} &= [x \quad y \quad \theta_x \quad \theta_y]^T, \mathbf{x}_s = [x_1 \quad x_2 \quad x_5 \quad x_6]^T \\ \mathbf{x}_r &= [x_{1r} \quad x_{2r} \quad x_{5r} \quad x_{6r}]^T, \hat{\mathbf{x}} = [\hat{x}_1 \quad \hat{x}_2 \quad \hat{x}_5 \quad \hat{x}_6]^T \\ \mathbf{i} &= [i_1 \quad i_2 \quad i_5 \quad i_6]^T \end{aligned}$$

$$\mathbf{M} = \begin{bmatrix} m & 0 & 0 & 0 \\ 0 & m & 0 & 0 \\ 0 & 0 & I_d & 0 \\ 0 & 0 & 0 & I_d \end{bmatrix}, \mathbf{M}_1 = \begin{bmatrix} 0 & 0 & 0 & 0 \\ 0 & 0 & 0 & 0 \\ 0 & 0 & 0 & I_p \\ 0 & 0 & -I_p & 0 \end{bmatrix}$$

$$\mathbf{F} = \begin{bmatrix} F_1 & 0 & F_5 & 0 \\ 0 & F_2 & 0 & F_6 \\ 0 & -F_2 l_1 & 0 & F_6 l_2 \\ F_1 l_1 & 0 & -F_5 l_2 & 0 \end{bmatrix}, \mathbf{G} = \begin{bmatrix} -G_1 & 0 & -G_5 & 0 \\ 0 & -G_2 & 0 & -G_6 \\ 0 & G_2 l_1 & 0 & -G_6 l_2 \\ -G_1 l_1 & 0 & G_5 l_2 & 0 \end{bmatrix}, \mathbf{U}_i = \begin{bmatrix} m\epsilon\omega^2 \cos(\omega t + \phi) \\ m\epsilon\omega^2 \sin(\omega t + \phi) \\ -(I_d - I_p)\tau\omega^2 \sin(\omega t + \psi) \\ -(I_d - I_p)\tau\omega^2 \cos(\omega t + \psi) \end{bmatrix}$$

$$\hat{\mathbf{x}} = \mathbf{x}_s + \mathbf{x}_r \quad (4)$$

The shaft displacement at the center of gravity and the sensor position of the AMBs is given from the geometrical relation of the shaft as follows:

$$\begin{aligned} \mathbf{x} &= \mathbf{L}\mathbf{x}_s = \mathbf{L}(\hat{\mathbf{x}} - \mathbf{x}_r) \quad (5) \\ \mathbf{L} &= \frac{1}{l_1 + l_2} \begin{bmatrix} l_2 & 0 & l_1 & 0 \\ 0 & l_2 & 0 & l_1 \\ 0 & -1 & 0 & 1 \\ 1 & 0 & -1 & 0 \end{bmatrix} \end{aligned}$$

As we have assumed the controller of the AMB to be the PID controller, the control current of the AMB are described as follows:

$$\mathbf{i} = \mathbf{K}_D \dot{\hat{\mathbf{x}}} + \mathbf{K}_P \hat{\mathbf{x}} + \mathbf{K}_I \int \hat{\mathbf{x}} dt \quad (6)$$

where

$$\mathbf{K}_D = \begin{bmatrix} K_{D1} & 0 & 0 & 0 \\ 0 & K_{D2} & 0 & 0 \\ 0 & 0 & K_{D5} & 0 \\ 0 & 0 & 0 & K_{D6} \end{bmatrix}, \mathbf{K}_P = \begin{bmatrix} K_{P1} & 0 & 0 & 0 \\ 0 & K_{P2} & 0 & 0 \\ 0 & 0 & K_{P5} & 0 \\ 0 & 0 & 0 & K_{P6} \end{bmatrix}, \mathbf{K}_I = \begin{bmatrix} K_{I1} & 0 & 0 & 0 \\ 0 & K_{I2} & 0 & 0 \\ 0 & 0 & K_{I5} & 0 \\ 0 & 0 & 0 & K_{I6} \end{bmatrix}$$

Now we adopt the estimated values in table 1 as the controller gain  $k_{D_i}, K_{P_i}, K_{I_i}$  ( $i = 1, 2, 5, 6$ ).

Substituting equations (4)(5)(6) for  $\mathbf{x}_s, \mathbf{x}, \mathbf{i}$  of equation (3), we obtain a following equation of motion:

$$\mathbf{M}\mathbf{L}\ddot{\hat{\mathbf{x}}} + (\omega\mathbf{M}_1\mathbf{L} + \mathbf{F}\mathbf{K}_D)\dot{\hat{\mathbf{x}}} + (\mathbf{F}\mathbf{K}_P + \mathbf{G})\hat{\mathbf{x}} + \mathbf{F}\mathbf{K}_I \int \hat{\mathbf{x}} dt = \mathbf{U}_i + \mathbf{M}\mathbf{L}\ddot{\mathbf{x}}_r + \omega\mathbf{M}_1\mathbf{L}\dot{\mathbf{x}}_r + \mathbf{G}\mathbf{x}_r \quad (7)$$

The unbalance matrix  $\mathbf{U}_i$  is represented as follows:

$$\mathbf{U}_i = \omega^2 \mathbf{M}_2 \begin{bmatrix} \varepsilon \cos(\omega t + \phi) \\ \varepsilon \sin(\omega t + \phi) \\ -\tau \sin(\omega t + \psi) \\ \tau \cos(\omega t + \psi) \end{bmatrix} \quad (8)$$

where

$$\mathbf{M}_2 = \begin{bmatrix} m & 0 & 0 & 0 \\ 0 & m & 0 & 0 \\ 0 & 0 & I_d - I_p & 0 \\ 0 & 0 & 0 & I_d - I_p \end{bmatrix}$$

$\varepsilon, \phi$  are mass eccentricity and its phase,  $\tau, \psi$  are inclination of the central principal axis of inertia and its phase and  $\omega$  is rotating speed.

The sensor runout vector  $\mathbf{x}_r$  is represented as follows:

$$\mathbf{x}_r = \begin{bmatrix} \lambda_1 \cos(\omega t + \phi_1) \\ \lambda_1 \sin(\omega t + \phi_1) \\ \lambda_2 \cos(\omega t + \phi_2) \\ \lambda_2 \sin(\omega t + \phi_2) \end{bmatrix} \quad (9)$$

where  $\lambda, \phi$  are the sensor runout and its phase and subscripts 1,2 identify 2 radial bearings.

### 3. IDENTIFICATION METHOD

The identification method is as follows:

#### (1). Laplace transforms of the Equation of motion

Taking Laplace transforms of equation (7), we obtain the left-hand term of the equation as

$$\left[ \mathbf{M}\mathbf{L}s^2 + (\omega\mathbf{M}_1\mathbf{L} + \mathbf{F}\mathbf{K}_D)s + (\mathbf{F}\mathbf{K}_P + \mathbf{G}) + \mathbf{F}\mathbf{K}_I \frac{1}{s} \right] \hat{\mathbf{X}}(s)$$

where  $L[\bullet]$  is the Laplace transforms and  $L(\hat{\mathbf{x}}) = \hat{\mathbf{X}}(s)$ .

The right-hand term of equation (7) by the Laplace transforms is given as follows:

#### First term of the right-hand term

$$L[\mathbf{U}_i] = \frac{\omega^2}{s^2 + \omega^2} \mathbf{M}_2 \begin{bmatrix} \varepsilon(s \cos \phi - \omega \sin \phi) \\ \varepsilon(\omega \cos \phi + s \sin \phi) \\ -\tau(\omega \cos \psi + s \sin \psi) \\ \tau(s \cos \psi - \omega \sin \psi) \end{bmatrix} = U(s) \omega \mathbf{M}_2 \begin{bmatrix} s & -\omega & 0 & 0 \\ \omega & s & 0 & 0 \\ 0 & 0 & -\omega & -s \\ 0 & 0 & s & -\omega \end{bmatrix} \begin{bmatrix} \varepsilon \cos \phi \\ \varepsilon \sin \phi \\ \tau \cos \psi \\ \tau \sin \psi \end{bmatrix}$$

$$= \mathbf{M}_2 \left[ s\omega \begin{bmatrix} 1 & 0 & 0 & 0 \\ 0 & 1 & 0 & 0 \\ 0 & 0 & 0 & -1 \\ 0 & 0 & 1 & 0 \end{bmatrix} + \omega^2 \begin{bmatrix} 0 & -1 & 0 & 0 \\ 1 & 0 & 0 & 0 \\ 0 & 0 & -1 & 0 \\ 0 & 0 & 0 & -1 \end{bmatrix} \right] U(s) \mathbf{E} = \mathbf{M}_2 [s\omega \mathbf{H}_{01} + \omega^2 \mathbf{H}_{02}] U(s) \mathbf{E}$$

where

$$U(s) = L[\sin(\omega t)] = \frac{\omega}{s^2 + \omega^2}, \quad \mathbf{E} = \begin{bmatrix} \mathbf{E}_0 \\ \mathbf{E}_1 \end{bmatrix}; \quad \mathbf{E}_0 = \begin{bmatrix} \varepsilon \cos \phi \\ \varepsilon \sin \phi \\ \tau \cos \psi \\ \tau \sin \psi \end{bmatrix}, \quad \mathbf{E}_1 = \begin{bmatrix} \lambda_1 \cos \phi_1 \\ \lambda_1 \sin \phi_1 \\ \lambda_2 \cos \phi_2 \\ \lambda_2 \sin \phi_2 \end{bmatrix}$$

$$\mathbf{H}_{01} = \begin{bmatrix} 1 & 0 & 0 & 0 \\ 0 & 1 & 0 & 0 \\ 0 & 0 & 0 & -1 \\ 0 & 0 & 1 & 0 \end{bmatrix}, \quad \mathbf{H}_{02} = \begin{bmatrix} 0 & -1 & 0 & 0 \\ 1 & 0 & 0 & 0 \\ 0 & 0 & -1 & 0 \\ 0 & 0 & 0 & -1 \end{bmatrix}$$

$\mathbf{0}$  is  $4 \times 4$  zero matrix.

### Second term of the right-hand term

$$\mathbf{M} \mathbf{L} \mathbf{L} [\ddot{\mathbf{x}}_r] = \frac{-\omega^2}{s^2 + \omega^2} \mathbf{M} \mathbf{L} \begin{bmatrix} \lambda_1 (s \cos \phi_1 - \omega \sin \phi_1) \\ \lambda_1 (\omega \cos \phi_1 + s \sin \phi_1) \\ \lambda_2 (s \cos \phi_2 - \omega \sin \phi_2) \\ \lambda_2 (\omega \cos \phi_2 + s \sin \phi_2) \end{bmatrix} = \mathbf{M} \mathbf{L} [s\omega \mathbf{H}_{11} + \omega^2 \mathbf{H}_{12}] U(s) \mathbf{E}$$

where

$$\mathbf{H}_{11} = \begin{bmatrix} -1 & 0 & 0 & 0 \\ 0 & -1 & 0 & 0 \\ 0 & 0 & -1 & 0 \\ 0 & 0 & 0 & -1 \end{bmatrix}, \quad \mathbf{H}_{12} = \begin{bmatrix} 0 & 1 & 0 & 0 \\ -1 & 0 & 0 & 0 \\ 0 & 0 & 0 & 1 \\ 0 & 0 & -1 & 0 \end{bmatrix}$$

### Third term of the right-hand term

$$\omega \mathbf{M}_1 \mathbf{L} \mathbf{L} [\dot{\mathbf{x}}_r] = \frac{\omega^2}{s^2 + \omega^2} \mathbf{M}_1 \mathbf{L} \begin{bmatrix} -\lambda_1 (\omega \cos \phi_1 + s \sin \phi_1) \\ \lambda_1 (s \cos \phi_1 - \omega \sin \phi_1) \\ -\lambda_2 (\omega \cos \phi_2 + s \sin \phi_2) \\ \lambda_2 (s \cos \phi_2 - \omega \sin \phi_2) \end{bmatrix} = \omega U(s) \mathbf{M}_1 \mathbf{L} \begin{bmatrix} -\omega & -s & 0 & 0 \\ s & -\omega & 0 & 0 \\ 0 & 0 & -\omega & -s \\ 0 & 0 & s & -\omega \end{bmatrix} \mathbf{E}_1$$

$$= \omega \mathbf{M}_1 \mathbf{L} [s\mathbf{H}_{21} + \omega \mathbf{H}_{22}] U(s) \mathbf{E}$$

where

$$\mathbf{H}_{21} = \begin{bmatrix} 0 & -1 & 0 & 0 \\ 1 & 0 & 0 & 0 \\ 0 & 0 & 0 & -1 \\ 0 & 0 & 1 & 0 \end{bmatrix}, \quad \mathbf{H}_{22} = \begin{bmatrix} -1 & 0 & 0 & 0 \\ 0 & -1 & 0 & 0 \\ 0 & 0 & -1 & 0 \\ 0 & 0 & 0 & -1 \end{bmatrix}$$

Fourth term of the right-hand term

$$\begin{aligned} \mathbf{GL}[\mathbf{x}_r] &= \frac{1}{s^2 + \omega^2} \mathbf{G} \begin{bmatrix} \lambda_1 (s \cos \phi_1 - \omega \sin \phi_1) \\ \lambda_1 (\omega \cos \phi_1 + s \sin \phi_1) \\ \lambda_2 (s \cos \phi_2 - \omega \sin \phi_2) \\ \lambda_2 (\omega \cos \phi_2 + s \sin \phi_2) \end{bmatrix} = \frac{U(s)}{\omega} \mathbf{G} \begin{bmatrix} s & -\omega & 0 & 0 \\ \omega & s & 0 & 0 \\ 0 & 0 & s & -\omega \\ 0 & 0 & \omega & s \end{bmatrix} \mathbf{E}_1 \\ &= \mathbf{G} \left[ s \frac{1}{\omega} \mathbf{H}_{31} + \mathbf{H}_{32} \right] U(s) \mathbf{E} \end{aligned}$$

where

$$\mathbf{H}_{31} = \begin{bmatrix} 1 & 0 & 0 & 0 \\ 0 & 1 & 0 & 0 \\ 0 & 0 & 1 & 0 \\ 0 & 0 & 0 & 1 \end{bmatrix}, \quad \mathbf{H}_{32} = \begin{bmatrix} 0 & -1 & 0 & 0 \\ 1 & 0 & 0 & 0 \\ 0 & 0 & 0 & -1 \\ 0 & 0 & 1 & 0 \end{bmatrix}$$

In the end, we obtain the Laplace transforms of equation (7) as follows:

$$\left[ \mathbf{M}Ls^2 + (\omega\mathbf{M}_1L + \mathbf{F}K_D)s + (\mathbf{F}K_P + \mathbf{G}) + \mathbf{F}K_I \frac{1}{s} \right] \hat{\mathbf{X}}(s) = [\mathbf{H}_1(\omega)s + \mathbf{H}_2(\omega)]U(s)\mathbf{E} \quad (11)$$

where

$$\mathbf{H}_1(\omega) = \omega\mathbf{M}_2\mathbf{H}_{01} + \omega\mathbf{M}L\mathbf{H}_{11} + \omega\mathbf{M}_1L\mathbf{H}_{21} + \frac{1}{\omega}\mathbf{G}\mathbf{H}_{31}$$

$$\mathbf{H}_2(\omega) = \omega^2\mathbf{M}_2\mathbf{H}_{02} + \omega^2\mathbf{M}L\mathbf{H}_{12} + \omega^2\mathbf{M}_1L\mathbf{H}_{22} + \mathbf{G}\mathbf{H}_{32}$$

(2) Discrete-time system from continuous time system using the Bilinear z transformation

Substituting equation (12) to equation (11) to take the bilinear z transform of equation.(11) , we obtain the equation in the z plane as equation (13):

$$s = 2(1 - z^{-1})/T(1 + z^{-1}) \quad (12)$$

$$[\mathbf{W}_0 + \mathbf{W}_1z^{-1} + \mathbf{W}_2z^{-2} + \mathbf{W}_3z^{-3}] \hat{\mathbf{X}}(z) = [\mathbf{U}_0 + \mathbf{U}_1z^{-1} + \mathbf{U}_2z^{-2} + \mathbf{U}_3z^{-3}]U(z)\mathbf{E} \quad (13)$$

where

$$\begin{cases} \mathbf{W}_0 = 8\mathbf{M}L + 4T(\omega\mathbf{M}_1L + \mathbf{F}K_D) + 2T^2(\mathbf{F}K_P + \mathbf{G}) + T^3\mathbf{F}K \\ \mathbf{W}_1 = -24\mathbf{M}L - 4T(\omega\mathbf{M}_1L + \mathbf{F}K_D) + 2T^2(\mathbf{F}K_P + \mathbf{G}) + 3T^3\mathbf{F}K \\ \mathbf{W}_2 = 24\mathbf{M}L - 4T(\omega\mathbf{M}_1L + \mathbf{F}K_D) - 2T^2(\mathbf{F}K_P + \mathbf{G}) + 3T^3\mathbf{F}K \\ \mathbf{W}_3 = -8\mathbf{M}L + 4T(\omega\mathbf{M}_1L + \mathbf{F}K_D) - 2T^2(\mathbf{F}K_P + \mathbf{G}) + T^3\mathbf{F}K \end{cases}$$



$$\begin{cases} U_0 = 4TH_1(\omega) + 2T^2H_2(\omega) \\ U_1 = -4TH_1(\omega) + 2T^2H_2(\omega) \\ U_2 = -4TH_1(\omega) - 2T^2H_2(\omega) \\ U_3 = 4TH_1(\omega) - 2T^2H_2(\omega) \end{cases}$$

$T$  is the sampling period

As  $z$  is unit delay, following relations are given:

$$\begin{aligned} z^{-i}\hat{\mathbf{X}}_k(z) &= \mathbf{X}_{k-i}(z) = \hat{\mathbf{x}}(k-i) \\ z^{-i}U_k(z) &= U_{k-i}(z) = u(k-i) \end{aligned}$$

Substituting the upper equations to equation (13), we obtain the equation in the discrete-time system

$$\begin{aligned} & \mathbf{W}_0\hat{\mathbf{x}}(k) + \mathbf{W}_1\hat{\mathbf{x}}(k-1) + \mathbf{W}_2\hat{\mathbf{x}}(k-2) + \mathbf{W}_3\hat{\mathbf{x}}(k-3) \\ &= [\mathbf{U}_0u(k) + \mathbf{U}_1u(k-1) + \mathbf{U}_2u(k-2) + \mathbf{U}_3u(k-3)]\mathbf{E} \end{aligned} \quad (14)$$

Replacing the left-hand term and the parenthesized term in the right-hand term of equation (14) by  $\mathbf{W}(k)$ ,  $\mathbf{U}(k)$  and substituting  $\mathbf{W}(k)$ ,  $\mathbf{U}(k)$  to equation (14), we obtain equation (15).

$$\begin{aligned} \mathbf{W}(k) &= \mathbf{W}_0\mathbf{x}(k) + \mathbf{W}_1\mathbf{x}(k-1) + \mathbf{W}_2\mathbf{x}(k-2) + \mathbf{W}_3\mathbf{x}(k-3) \quad \mathbf{U}(k) = \mathbf{U}_0u(k) + \mathbf{U}_1u(k-1) + \mathbf{U}_2u(k-2) + \mathbf{U}_3u(k-3) \\ \mathbf{W}(k) &= \mathbf{U}(k)\mathbf{E} \quad (k=1 \dots n) \end{aligned} \quad (15)$$

In equation (15), the left-hand term  $\mathbf{W}(k)$  is determined from the dynamic parameters of the rotor and AMB, the sampling period and the measured shaft displacement including the sensor runout and also the  $\mathbf{U}(k)$  in the right-hand term is determined from the dynamic parameters of the rotor and AMB, the sampling period and the rotating speed.  $\mathbf{E}$  is an unknown vector, of which element are unknown unbalance and sensor runout and can be identified by the incremental least-square method.

### (3) the incremental least-square method.

As we may use  $n$  sets of  $\mathbf{W}(k)$ ,  $\mathbf{U}(k)$  ( $k=1 \dots n$ ) and get  $4n$  equations in equation (16) to identify the unknown vector  $\mathbf{E}$  so that we employ the incremental least-square method to estimate the unbalance and the sensor runout.

$$\mathbf{W} = \mathbf{U}\mathbf{E} \quad (16)$$

where

$$\mathbf{W} = [\mathbf{W}(1) \quad \mathbf{W}(2) \quad \dots \quad \mathbf{W}(n)]^T, \quad \mathbf{U} = [\mathbf{U}(1) \quad \mathbf{U}(2) \quad \dots \quad \mathbf{U}(n)]^T$$

In order to minimize the estimation error, a following quadratic cost function  $J$  is introduced and  $\mathbf{E}$  is determined by minimizing the cost function  $J$ .

$$J = \mathbf{R}^T \mathbf{R}$$

where  $\mathbf{R} = \mathbf{W} - \mathbf{U}\mathbf{E}$  is the estimation error.

Its minimum satisfies

$$\frac{\partial J}{\partial \mathbf{E}} = -2\mathbf{U}^T \mathbf{W} + 2\mathbf{U}^T \mathbf{U} \mathbf{E} = 0$$

, which gives

$$\mathbf{E} = (\mathbf{U}^T \mathbf{U})^{-1} \mathbf{U}^T \mathbf{W}$$

provided of course the inverse  $(\mathbf{U}^T \mathbf{U})^{-1}$  exists.

The incremental least square on-line method is applied to identify. The incremental least square on-line algorithm<sup>13,14)</sup> is given as follows:

$$\hat{\mathbf{E}}(k) = \hat{\mathbf{E}}(k-1) + \mathbf{P}(k) \mathbf{U}^T(k) \mathbf{q}(k) \quad (17)$$

where

$$\begin{aligned} \mathbf{q}(k) &= \mathbf{W}(k) - \mathbf{U}(k) \hat{\mathbf{E}}(k-1), \quad \mathbf{Q}(k) = [\mathbf{I} + \mathbf{U}(k) \mathbf{P}(k-1) \mathbf{U}^T(k)]^{-1} \\ \mathbf{P}(k) &= \mathbf{P}(k-1) - \mathbf{P}(k-1) \mathbf{U}^T(k) \mathbf{Q}(k) \mathbf{U}(k) \mathbf{P}(k-1) \end{aligned}$$

## 5. IDENTIFICATION RESULTS USING SIMULATION DATA

Numerical simulation of the rotor vibration excited by the unbalance and levitated by the AMB including the measurement error caused by the AMB sensor runout is carried out to evaluate the proposed method for estimation of the unbalance and the sensor runout on the rotor. The Runge-Kutta method is employed and the condition of the numerical simulation is tabulated in table 2. 1000 data on the rotor displacement are calculated at each bearing at 500rpm and 1500rpm. Sampling period is set to be 1.7msec. The calculated vibrations at both bearings are shown in figure 5

Table. 2 Condition of numerical simulation

	Rotating speed (rpm)	Sampling period (m sec)	Number of data
First data	500	1.7	500
Second data	1500	1.7	500

The unbalance and the sensor runout are identified by the algorithm in equation (17) using the simulated vibration data. The convergent process of the identification of the unbalance and the sensor runout is shown in figure 6. In this figure, the left side figures and the right side figures show the amplitude and the phase angles of the unbalance and the sensor runout respectively and the abscissa shows sampled data number. Solid lines indicate the identified values of the identifying parameters and dotted straight lines are given values, namely static unbalance  $\varepsilon = 2.0 \mu\text{m}$ , coupled unbalance  $\tau = 0.6 \times 10^{-4} \text{rad}$ , sensor runout of bearing 1  $\lambda_1 = 1.1 \mu\text{m}$  and sensor runout of bearing 2  $\lambda_2 = 2.2 \mu\text{m}$ .

Just after a change of the rotating speed from 500rpm to 1500rpm, all gains and phase angles of the identified parameters converge to the given values rapidly. From this numerical result, we confirm that the unbalance and the sensor runout on the AMB rotor may be identified by the proposed rotor model and the incremental least-square method.

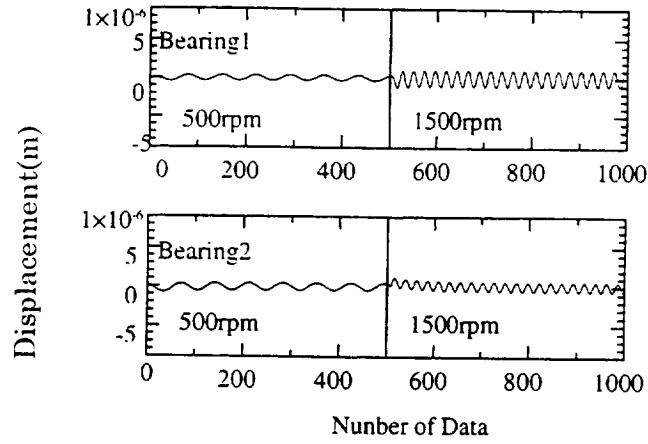


Fig.5 Time series data of calculated rotor displacement

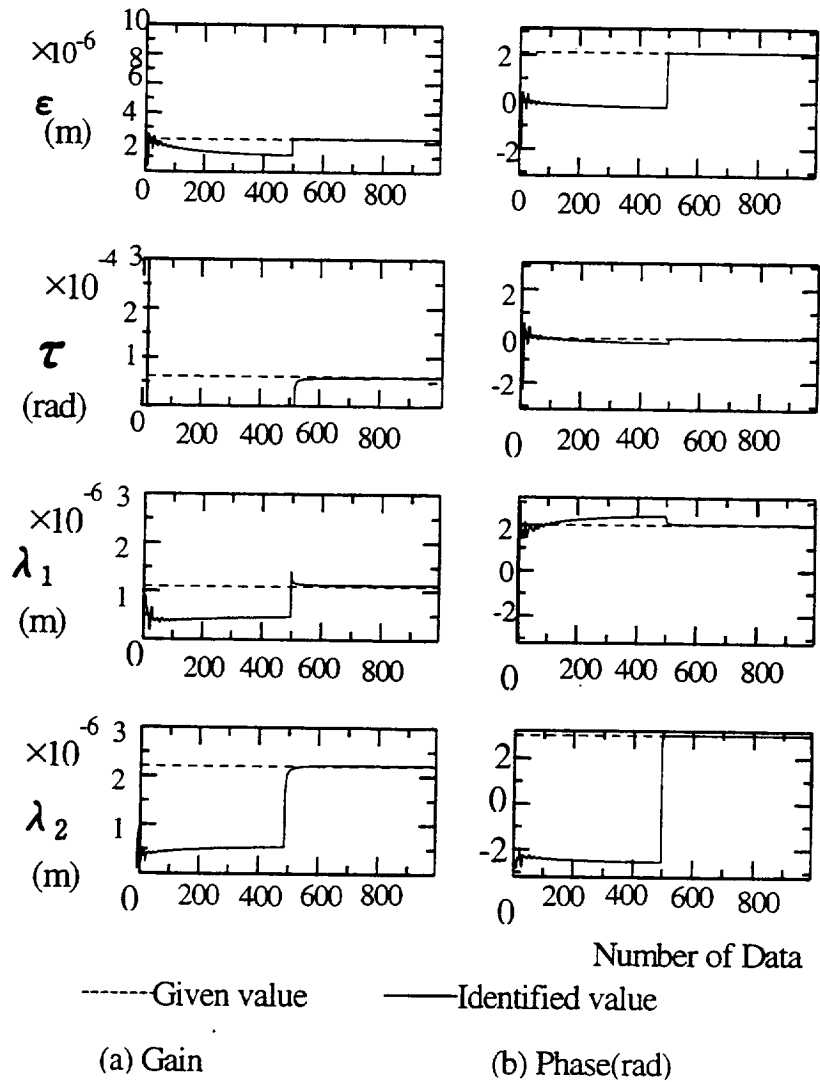


Fig 6 Identification process using the numerical simulation results.

## 6. IDENTIFICATION RESULTS USING MEASURED DATA OF TMP ROTOR

Figure 7 shows measured rotor vibration at the upper bearing(1) and the lower bearing(2) at 496rpm and 1498rpm. The sampling period is set to be 1.668ms and 1000 data of shaft vibration at both AMB are sampled and used for the identification.

In the figure these time series data seem to include high-order component caused by high-order component of the sensor runout. **But in this study, the high-order components in the vibration data are ignored and only the synchronous component of the sensor runout is identified in the identification algorithm because the effect of the high-order components of sensor runout does not have any effect on the synchronous vibration and the high-order component may be estimated separately.** We will propose a method for identifying the high-order component in next paper.

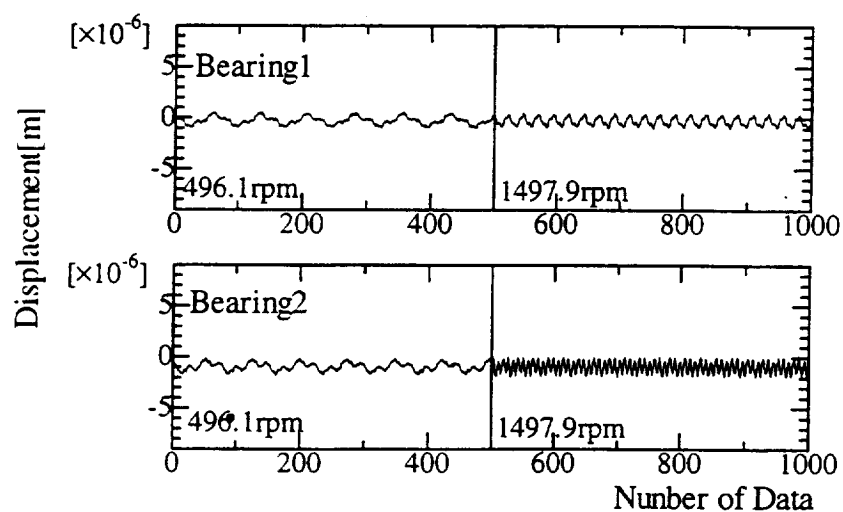


Fig. 7 Measured shaft vibration of the tested rotor before attaching trial weight

Table.3 Data of attached unbalance

Mass $m_0$ (g)	0.53
Distance from x axis $l_0$ (mm)	59.5
Distance from z axis $r_0$ (mm)	51.0

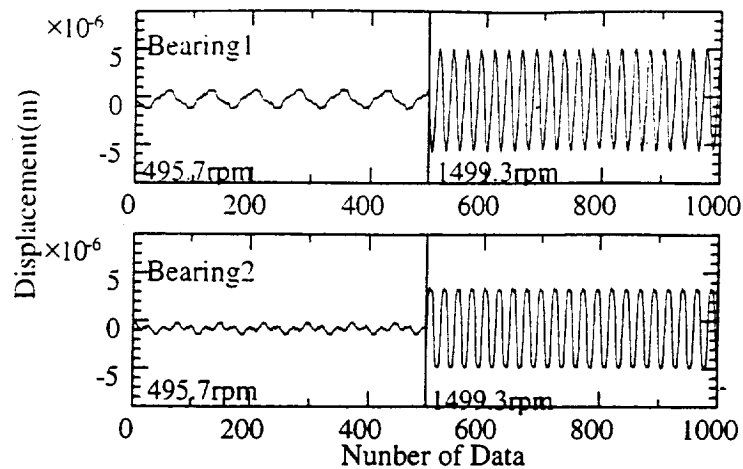


Fig. 8 Measured shaft vibration of the tested rotor after attaching trial weight

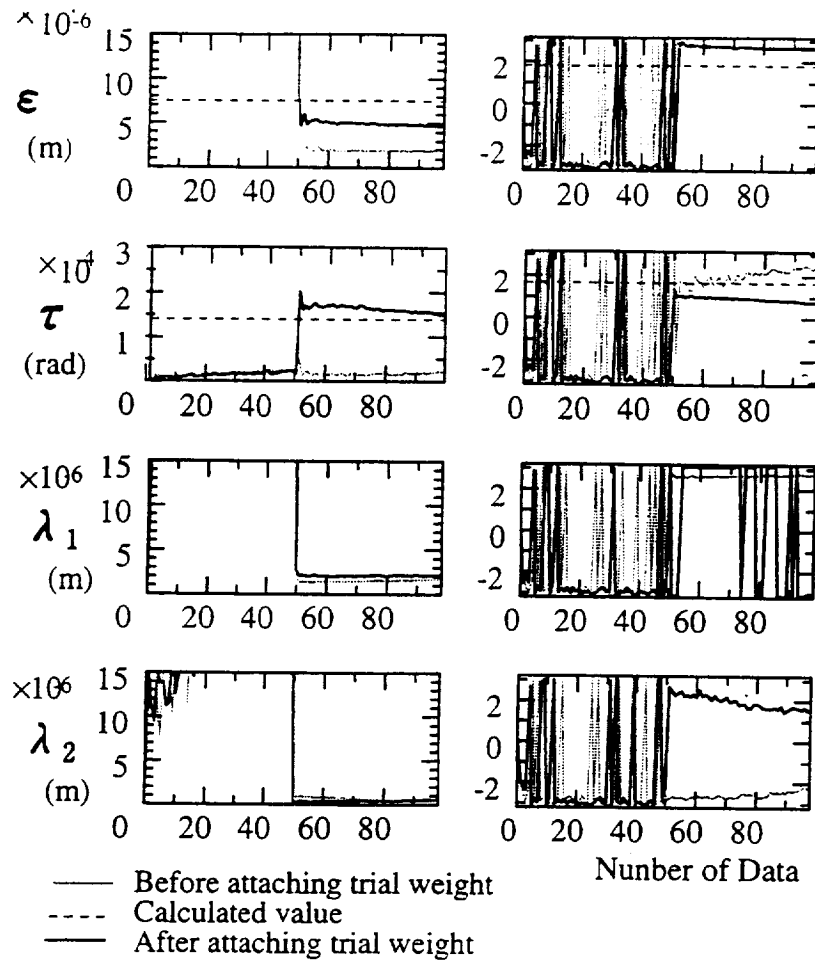
Figure 9 shows converging process of the identification of the static unbalance  $\varepsilon$ , coupled unbalance  $\tau$ , bearing1 runout  $\tau_1$  and bearing2 runout  $\tau_2$ . The identified gain and phase angle of the initial unbalance and the initial sensor runout are presented by slender solid lines in figure 9.

Unfortunately, we could not measure the initial unbalance of the tested rotor and the runout of the AMB sensor, so we try to identify the change of the unbalance between before and after attaching a known trial weight on outer surface of the dummy disk. The weight and the location of the attached unbalance is tabulated in table 3.

The measured time-series data of the vibration at the bearing 1 and 2 are measured in the same condition as figure 7 and are illustrated in figure 8. The identified gain and phase angle of the unbalance and the sensor runout are presented by bold solid lines in figure 9 using these data measured after attaching the trial weight.

In figure 9 dotted lines indicate the gain and phase angle of the parameters obtained by **vectorial** addition of the identified unbalance before attaching the weight and the attached weight so the difference between the bold solid lines and the dotted lines indicates the identification error. As we do not change the sensor runout especially so the estimated sensor runout after the attachment of the trial weight is reasonably same as before the attachment. In figure 9, the gains and the phase angles of  $\lambda_1$  and  $\lambda_2$  after attachment of the trial weight coincide with that before attachment so the sensor runout is identified correctly by the proposed method.

On the other hand as to the identification of the both unbalance  $\varepsilon$  and  $\tau$ , there is a slight difference between the bold solid lines and the dotted lines in figure 9.



(a) Gain

(b) Phase (rad)

Fig 9 Identification process using the experimental results.

## 7. CONCLUSIONS

We have developed the equation of motion of the rigid rotor supported by active magnetic bearings in consideration of the static and coupled unbalances and the sensor runout and proposed an identification method of the unbalance and the sensor runout simultaneously.

The numerical simulations and the experiments carried out here on unbalance response of the rotor have shown that the proposed method is effective for identifying the unbalance and the sensor runout on the AMB rotor.

## REFERENCES

- (1) Y.Kanemitsu, Non-contact Sensor of Shaft Vibration and its Problem, Journal of JSME, Vol.80, No.706,(1977)
- (2) Y.Kanemitsu, et.al., Real Time Balancing of a Flexible Rotor supported by magnetic bearing, proc. 2<sup>nd</sup> int. symp.on magnetic bearings,(1990)
- (3) S.Sagara, et al., System Identification, SICE (1981)
- (4) T.Nakamizo, Signal Analysis and System Identification, korona-sya (1988)
- (5) S.Beale, et al., Adaptive Forced Balancing for Magnetic Bearing Systems, Rproc. 3<sup>rd</sup> int. symp.on magnetic bearings (1992)